Science Advances
AAAS

Supplementary Materials for

NPRC deletion attenuates cardiac fibrosis in diabetic mice by activating PKA/PKG and inhibiting TGF-β1/Smad pathways

Linlin Meng *et al.*

Corresponding author: Yun Zhang, zhangyun@sdu.edu.cn; Cheng Zhang, zhangc@sdu.edu.cn

Sci. Adv. **9**, eadd4222 (2023)
DOI: 10.1126/sciadv.add4222

This PDF file includes:

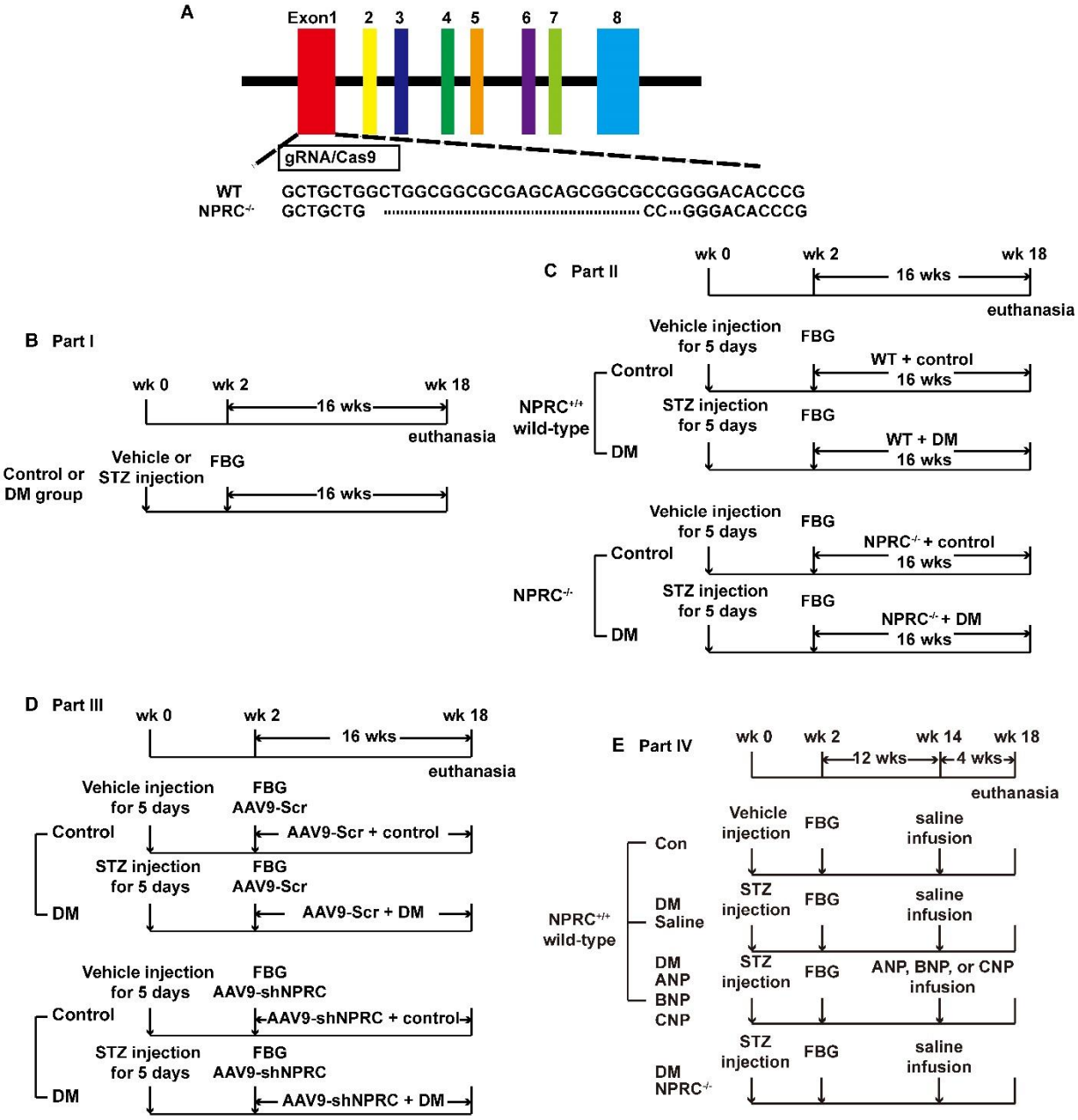

Fig. S1. Generation of NPRC$^{-/-}$ mice and time line of the *in vivo* experiments. (**A**) Schematic diagram of CRISPR/Cas9 for deletion of NPRC in mice. (**B-E**) Animal grouping and time line of the *in vivo* experiments. DM: diabetes mellitus; FBG: fasting blood glucose; wk: week.

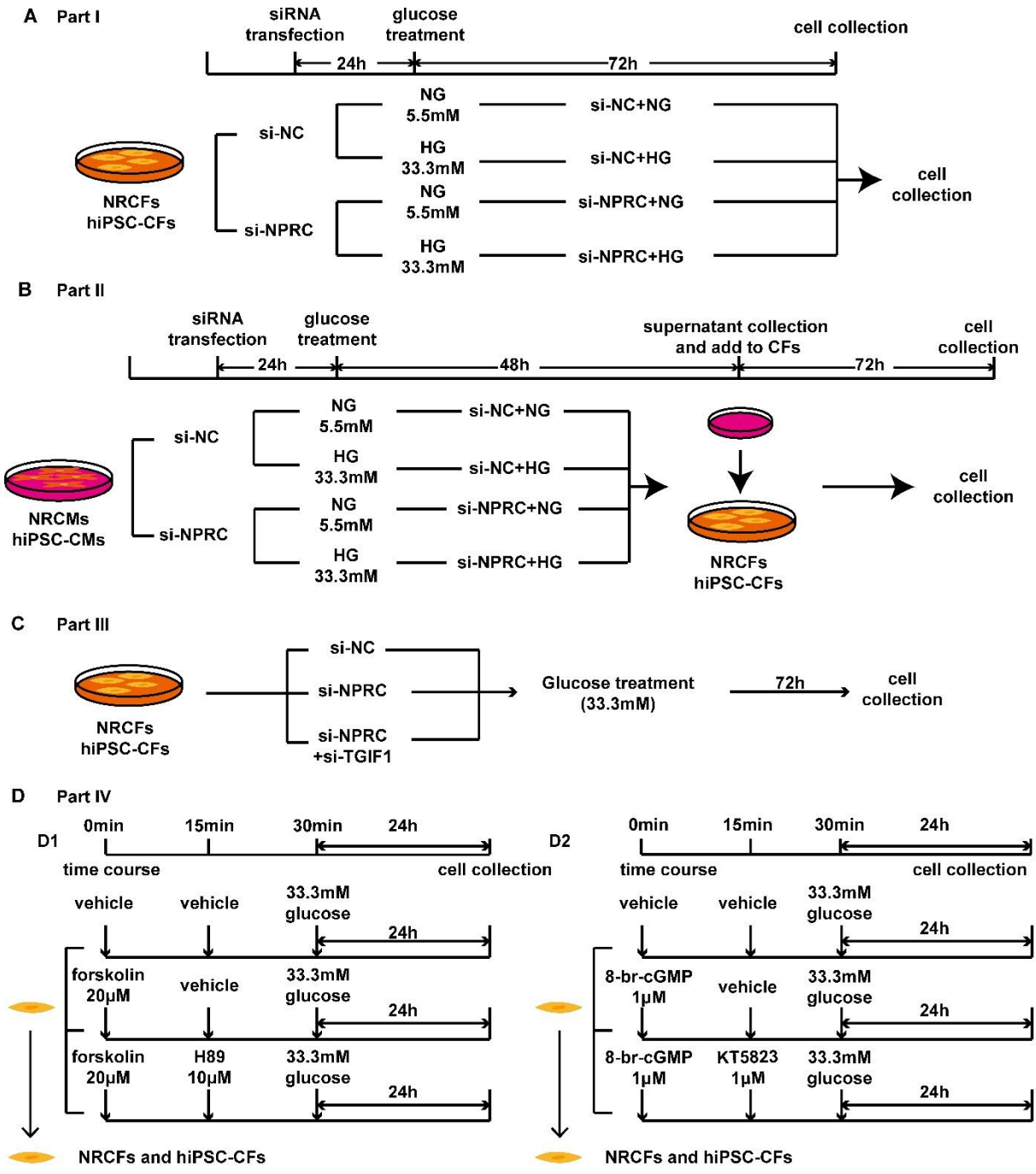

Fig. S2. Cell grouping and time line of the *in vitro* experiments. NG: normal glucose; HG: high glucose.

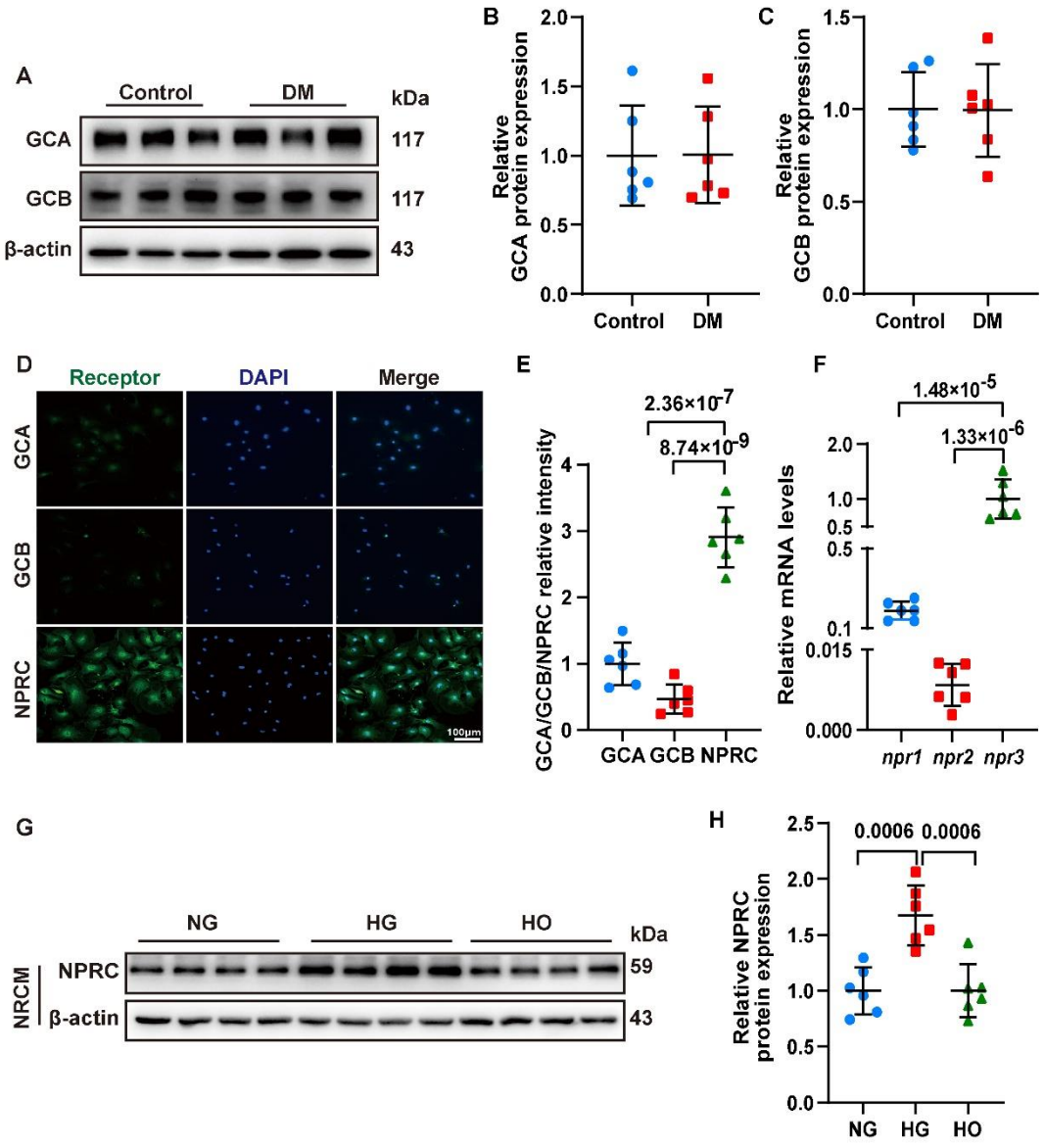

Fig. S3. GCA and GCB expression in the hearts of diabetic mice and NPRs distribution in CFs. (**A**) Representative Western blot images of GCA and GCB in the hearts from control or diabetic mice. (**B**) Quantification of the protein level of GCA in (**A**). n = 6 per group. (**C**) Quantification of the protein level of GCB in (**A**). n = 6 per group. (**D**) Representative immunofluorescence staining of GCA, GCB, and NPRC (green) in primary NRCFs. The nuclei were counterstained with DAPI (blue). Bar = 100 μm. (**E**) Quantification of the relative immunofluorescence intensity of GCA, GCB, and NPRC in (**D**). n = 6 per group. (**F**) Relative mRNA levels of *npr1*, *npr2*, and *npr3* in NRCFs. n = 6

per group. (**G**). Representative Western blot images of NPRC expression in NRCMs treated with normal concentration of glucose (NG), high concentration of glucose (HG) and high osmotic medium (HO). (**H**) Quantification of the protein expression of NPRC in (**G**). n = 6 per group. DM: diabetes mellitus. Normal distributions were tested by Shapiro-Wilk method. Unpaired two-tailed Student's t tests were applied in (**B**) and (**C**). One-way ANOVA was applied in (**E-F**) and (**H**).

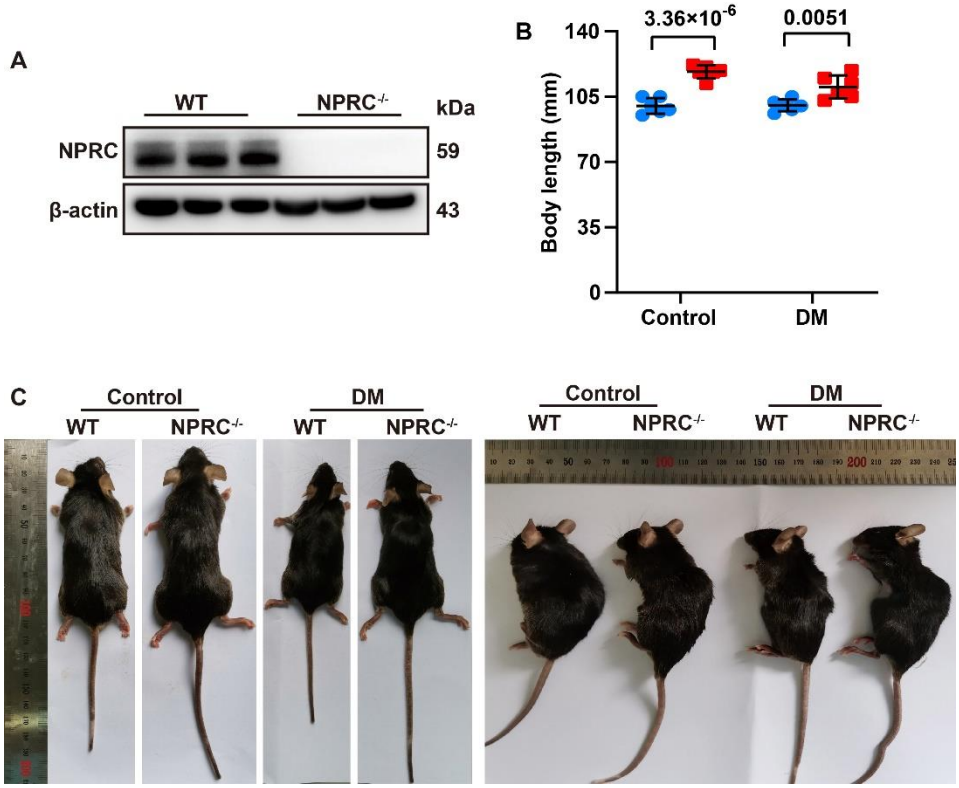

Fig. S4. General phenotypes of NPRC$^{-/-}$ mice. (**A**) Representative Western blot images of NPRC expression in the hearts of WT and NPRC$^{-/-}$ mice. (**B**) Comparison of body length among four groups of mice. n = 6 per group. (**C**) Representative photographs of WT and NPRC$^{-/-}$ mice in control and DM groups. Normal distributions were tested by Shapiro-Wilk method. Two-way ANOVA with Turkey's post-hoc test was used in (**B**).

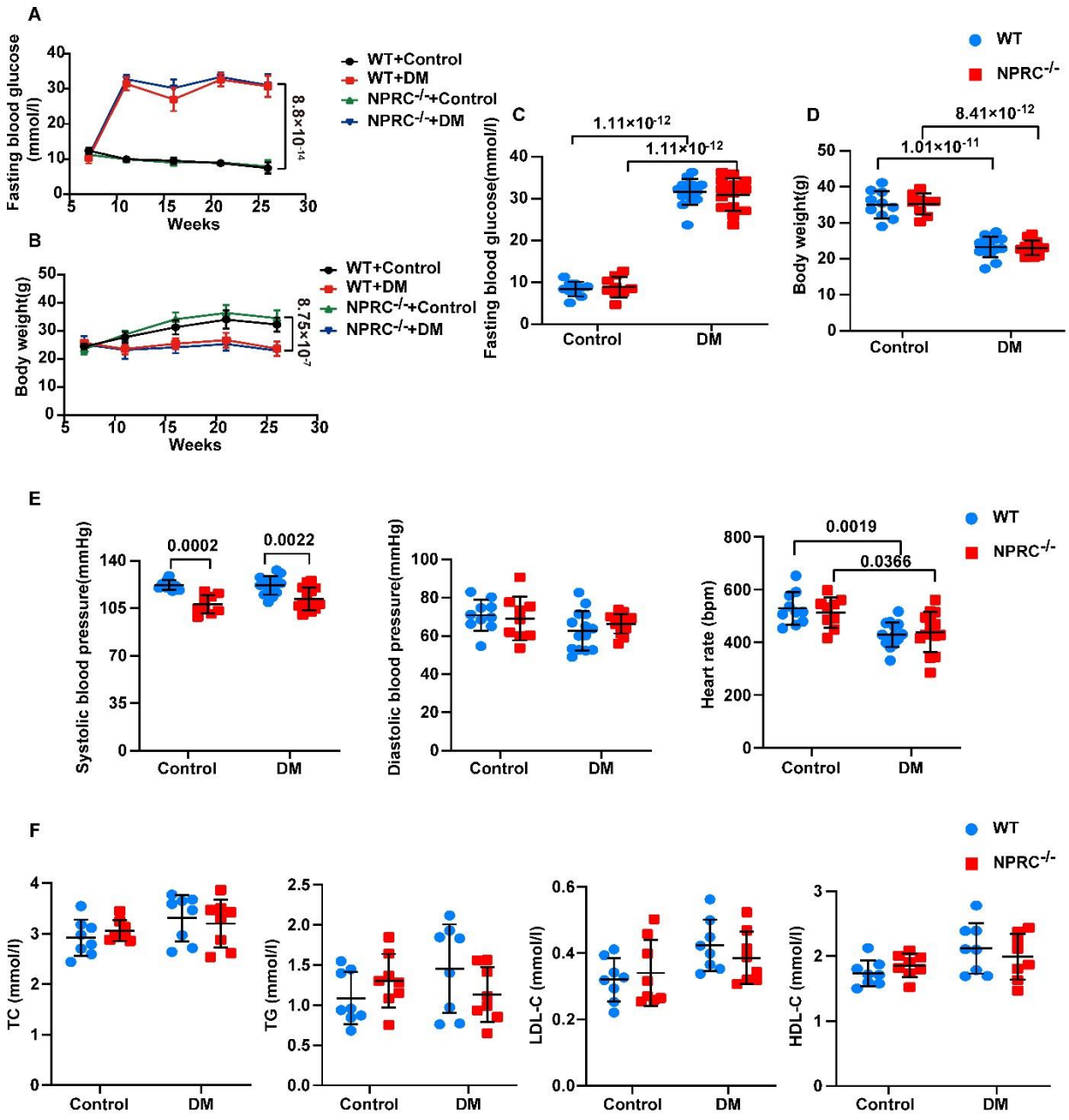

Fig. S5. Characterization of WT and NPRC$^{-/-}$ mice in control and DM groups. (**A**) Changes in fasting blood glucose in the four groups of mice during the experiment. n = 6 per group. (**B**) Changes in body weight in the four groups of mice during the experiment. n = 6 per group. (**C**) Comparison of fasting blood glucose among the four groups of mice before euthanasia. n = 9 to 14 per group. (**D**) Comparison of body weight among the four groups of mice before euthanasia. n = 9 to 14 per group. (**E**) Comparison of systolic blood

pressure, diastolic blood pressure, and heart rate among the four groups of mice. n = 9 to 14 per group. (**F**) Comparison of serum levels of total cholesterol (TC), triglycerides (TG), low-density lipoprotein cholesterol (LDL-C), and high-density lipoprotein cholesterol (HDL-C) among the four groups of mice. n = 8 per group. DM: diabetes mellitus; TC: total cholesterol; TG: triglycerides; LDL-C: low-density lipoprotein cholesterol; HDL-C: high-density lipoprotein cholesterol. Normal distributions were tested by Shapiro-Wilk method. Two-way ANOVA with Bonferroni post-hoc test was used in (**A-F**)**.**

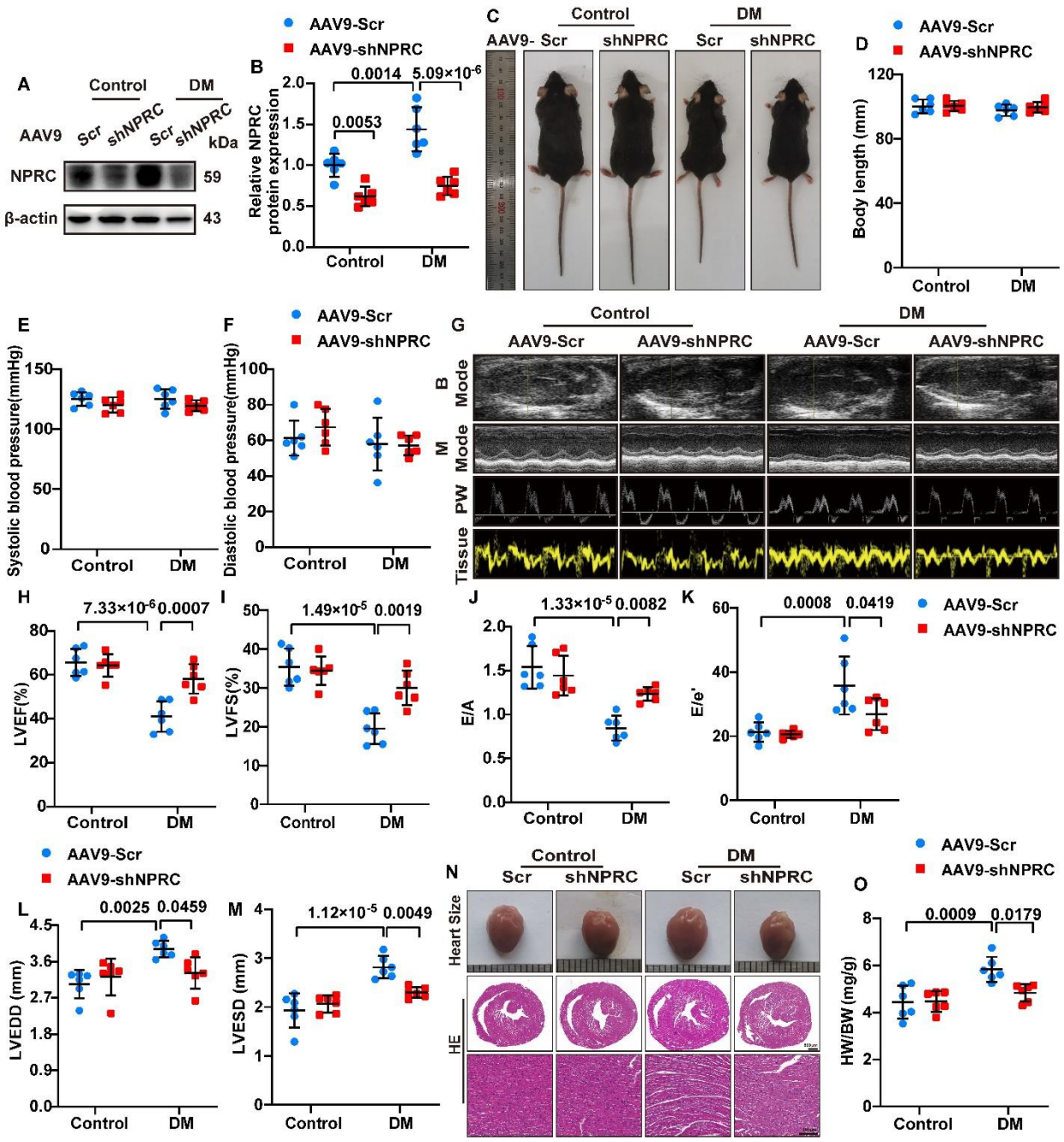

Fig. S6. Cardiac NPRC knockdown by AAV improved left ventricular function and remodeling in diabetic mice. (**A**) Representative Western blot images of NPRC in the hearts of four groups of AAV-delivered mice. (**B**) Quantification of the protein expression of NPRC in (**A**). n = 6 per group. (**C**) Representative photographs of AAV9-Scr or AAV9-shNPRC delivered mice in control and DM groups. (**D**) Comparison of body length among the four groups of mice. n = 6 per group. (**E**) Comparison of systolic blood pressure among

the four groups of mice. n = 6 per group. (**F**) Comparison of diastolic blood pressure among the four groups of mice. n = 6 per group. (**G**) Representative echocardiographic images for four groups of mice. B Mode represents a two-dimensional echocardiogram showing left ventricular long-axis view, M Mode represents M-mode echocardiogram showing left ventricular dimensions, PW represents pulse-wave Doppler spectrum depicting diastolic mitral flow, and Tissue represents tissue Doppler spectrum displaying mitral annular velocities. (**H**) Quantification of left ventricular ejection fraction (LVEF) in four groups of mice. n = 6 per group. (**I**) Quantification of left ventricular fractional shortening (LVFS) in four groups of mice. n = 6 per group. (**J**) Quantification of the ratio of early to late diastolic mitral flow velocities (E/A) in four groups of mice. n = 6 per group. (**K**) Quantification of the ratio of early diastolic mitral flow to early diastolic mitral annular velocities (E/e') in four groups of mice. n = 6 per group. (**L**) Quantification of left ventricular end-diastolic diameter (LVEDD) in four groups of mice. n = 6 per group. (**M**) Quantification of left ventricular end-systolic diameter (LVESD) in four groups of mice. n = 6 per group. (**N**) Representative photographs of the hearts from four groups of mice (the first row), cross-sectional images of hematoxylin and eosin (H&E) staining at the papillary muscle level of the hearts (the second row, bar = 500 μm), and H&E-stained sections of hearts from four groups of mice (the third row, bar = 100 μm). (**O**) Quantification of the ratio of heart weight (HW) to body weight (BW) in four groups of mice. n = 6 per group. PW: pulse-wave; DM: diabetes mellitus. Normal distributions were tested by Shapiro-Wilk method. Two-way ANOVA with Bonferroni post-hoc test was used in (**B**). Two-way ANOVA with Turkey's post-hoc test was used in (**D-F**), (**H-M**) and (**O**).

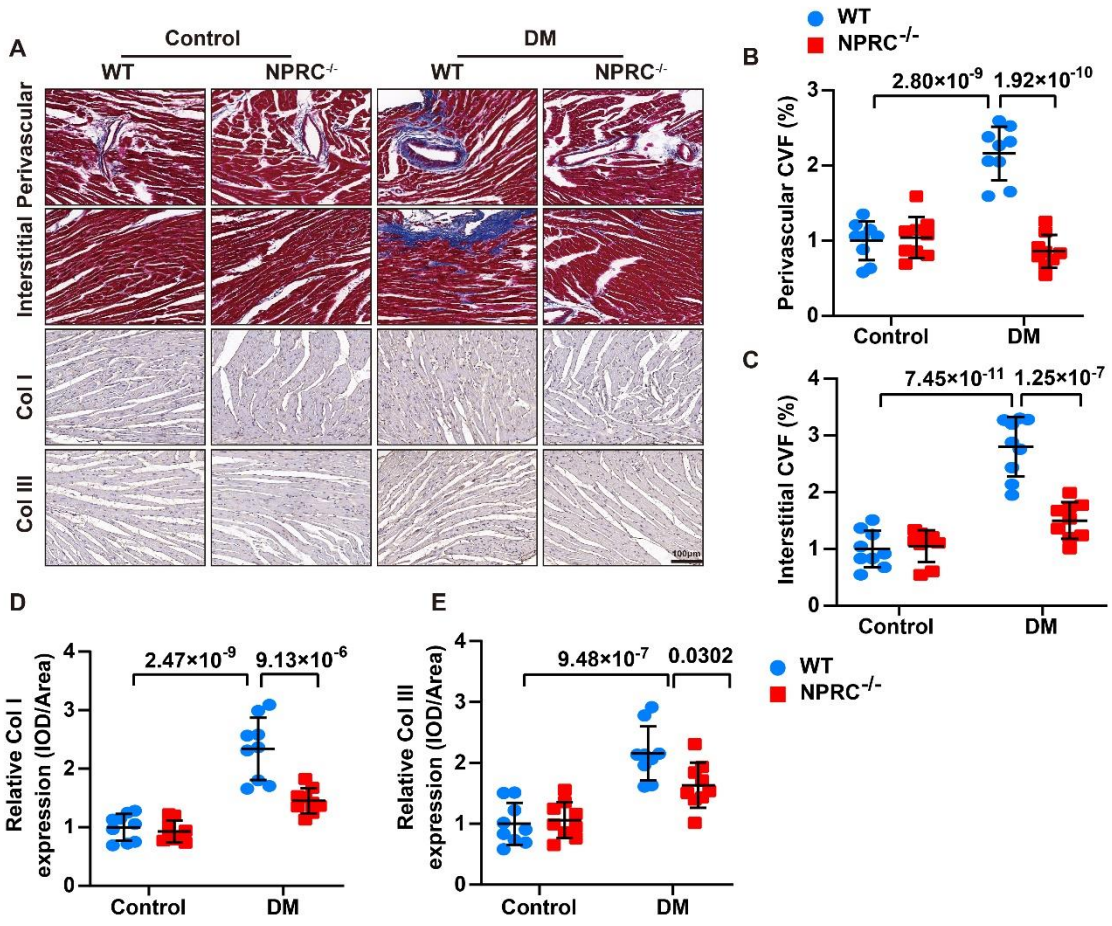

Fig. S7. NPRC deficiency alleviated left atrial fibrosis induced by diabetes *in vivo*. (**A**) Representative images of Masson's trichrome staining of the left atrial myocardium (the first and second row) and IHC of collagen I and collagen III in the left atrial myocardium (the third and fourth row) of four groups of mice. Bar = 100 μm. (**B-C**) Quantification of perivascular collagen volume fraction (CVF) and interstitial CVF in the left atrium of four groups of mice. n = 9 per group. (**D-E**) Quantification of IHC of collagen I and collagen III in the left atrium of four groups of mice. n = 9 per group. DM: diabetes mellitus. Normal distributions were tested by Shapiro-Wilk method. Two-way ANOVA with Turkey's post-hoc test was used in (**B-D**). Two-way ANOVA with Bonferroni post-hoc test was used in (**E**).

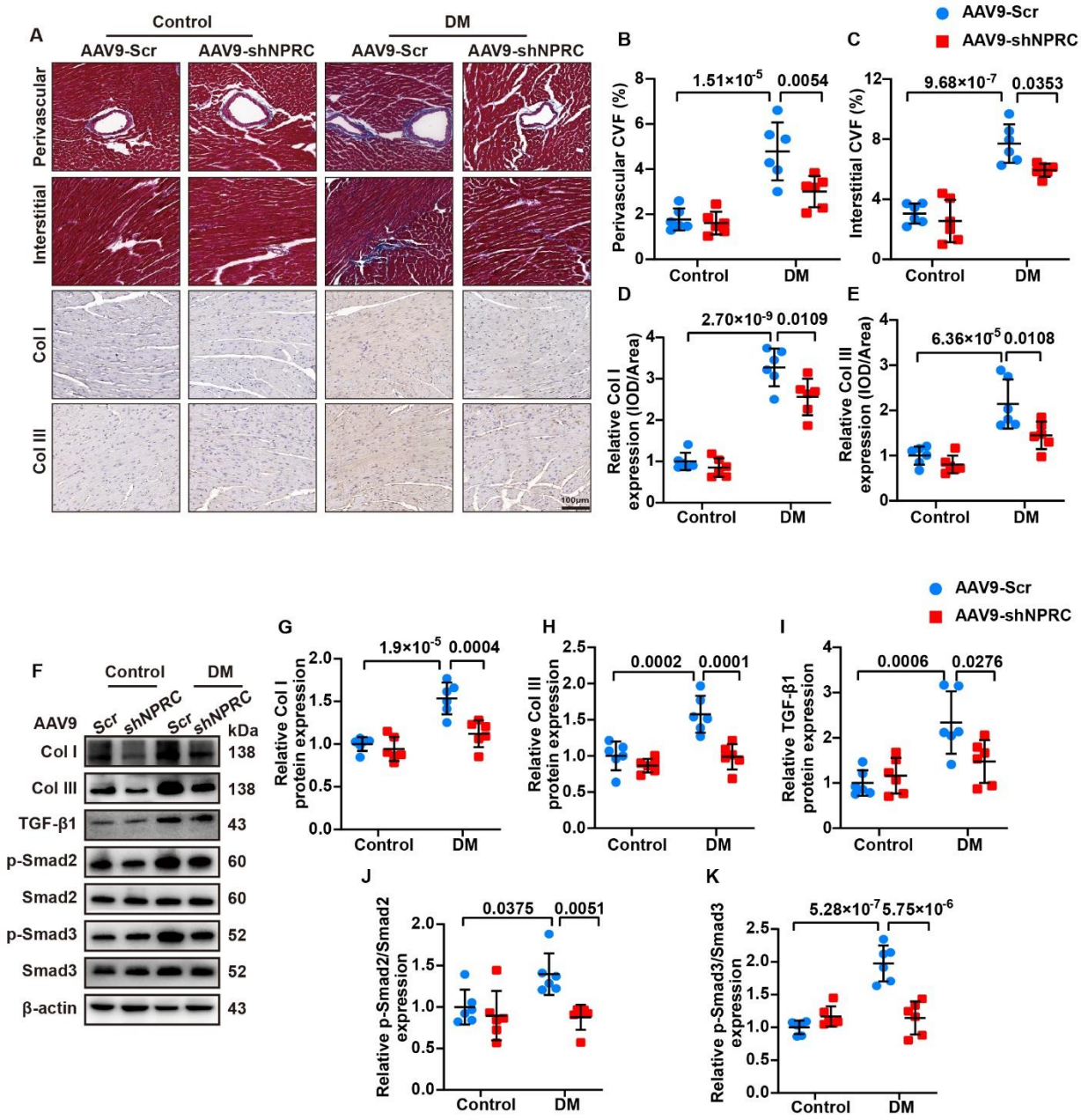

Fig. S8. Cardiac NPRC knockdown by AAV alleviated cardiac fibrosis induced by diabetes *in vivo*. (**A**)**.** Representative images of Masson's trichrome staining of the myocardium (the first and second row) and immunohistochemistry (IHC) of collagen I and collagen III in the myocardium (the third and fourth row) in four groups of AAV-delivered mice. Bar = 100 μm. (**B**)**.** Quantification of perivascular collagen volume fraction (CVF) in four groups of mice. n = 6 per group. (**C**) Quantification of interstitial CVF in four groups

of mice. n = 6 per group. (**D**) Quantification of IHC of collagen I in four groups of mice. n = 6 per group. (**E**) Quantification of IHC of collagen III in four groups of mice. n = 6 per group. (**F**) Representative Western blot images of collagen I, collagen III, TGF-β1, p-Smad2, and p-Smad3 in the hearts of four groups of mice. (**G-K**) Quantification of the protein expression of collagen I, collagen III, TGF-β1, p-Smad2, and p-Smad3 in (**F**). n = 6 per group. DM: diabetes mellitus; Col I: Collagen I; Col III: Collagen III; CVF: collagen volume fraction; IOD: integrated optical density. Normal distributions were tested by Shapiro-Wilk method. Two-way ANOVA with Bonferroni post-hoc test was used in (**B-E**) and (**G-K**).

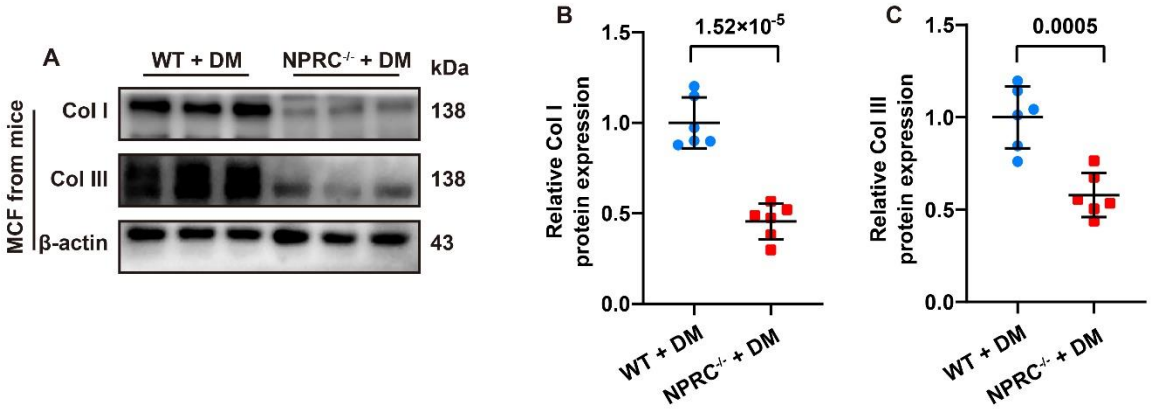

Fig. S9. NPRC deficiency decreased collagen synthesis in adult mouse CFs (MCFs). (A). Representative Western blot images of collagen I and collagen III of adult MCFs isolated from the hearts of diabetic WT and NPRC$^{-/-}$ mice. (**B-C**). Quantification of the protein expression of collagen I and collagen III in (**A**). n = 6 per group. DM: diabetes mellitus; Col I: Collagen I; Col III: Collagen III. Normal distributions were tested by Shapiro-Wilk method. Unpaired two-tailed Student's t tests were applied in (**B** and **C**).

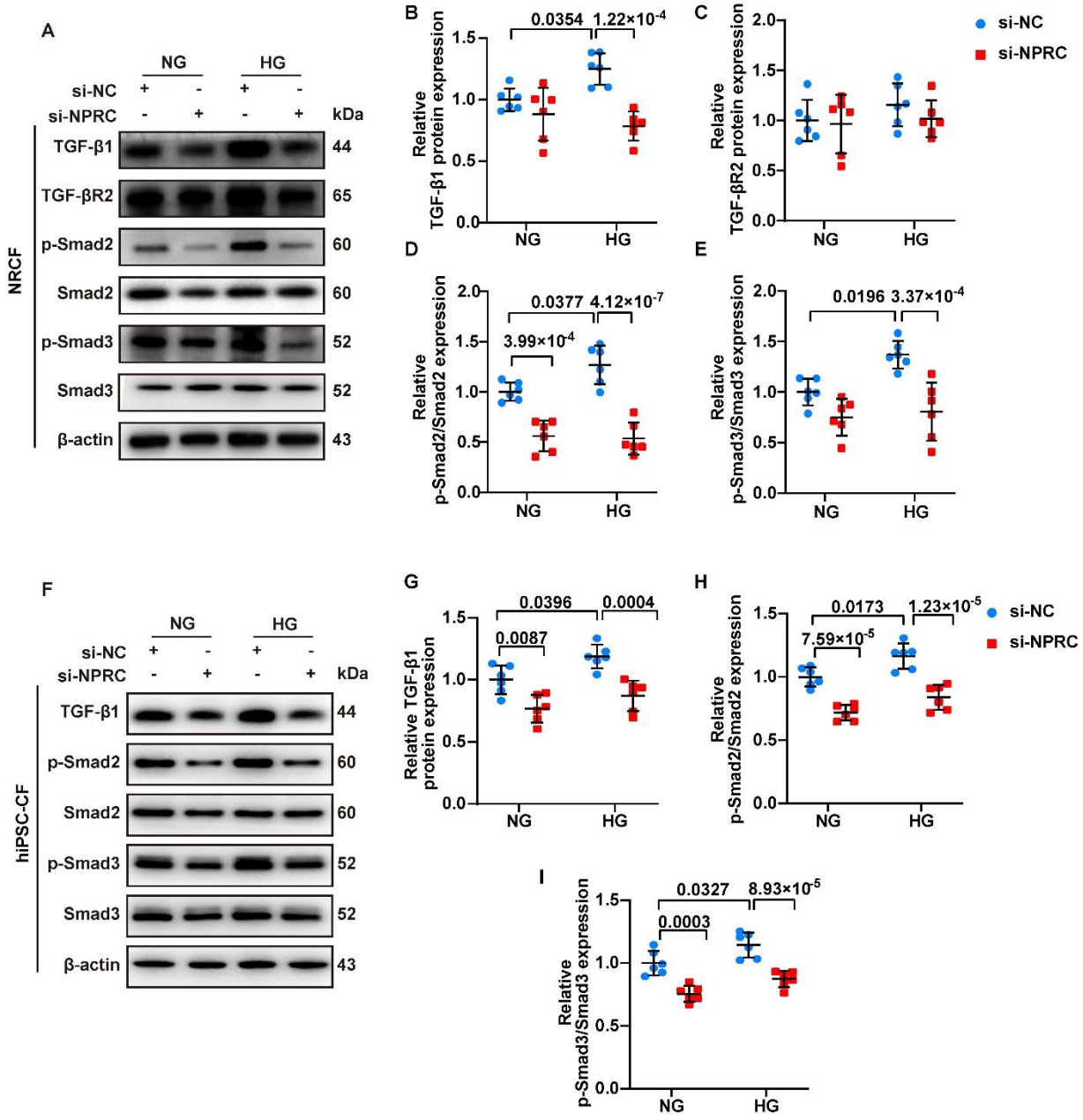

Fig. S10. NPRC deficiency inhibited TGF-β1/Smad signaling in CFs *in vitro*. (**A**) Representative Western blot images of TGF-β1, TGF-βR2, p-Smad2, and p-Smad3 expression in NRCFs transfected with si-NC or si-NPRC and treated with NG (5.5 mM) or HG (33.3 mM). (**B-E**) Quantification of the protein expression of TGF-β1, TGF-βR2, p-Smad2, and p-Smad3 in (**A**). n = 6 per group. (**F**) Representative Western blot images of TGF-β1, p-Smad2, and p-Smad3 expression in hiPSC-CFs transfected with si-NC or si-NPRC and treated with NG or HG. (**G-I**) Quantification of the protein expression of TGF-

β1, p-Smad2, and p-Smad3 in (**F**). n = 6 per group. NG: normal glucose; HG: high glucose. Normal distributions were tested by Shapiro-Wilk method. Two-way ANOVA with Turkey's post-hoc test was used in (**B, D**). Two-way ANOVA with Bonferroni post-hoc test was used in (**C, E, G-I**).

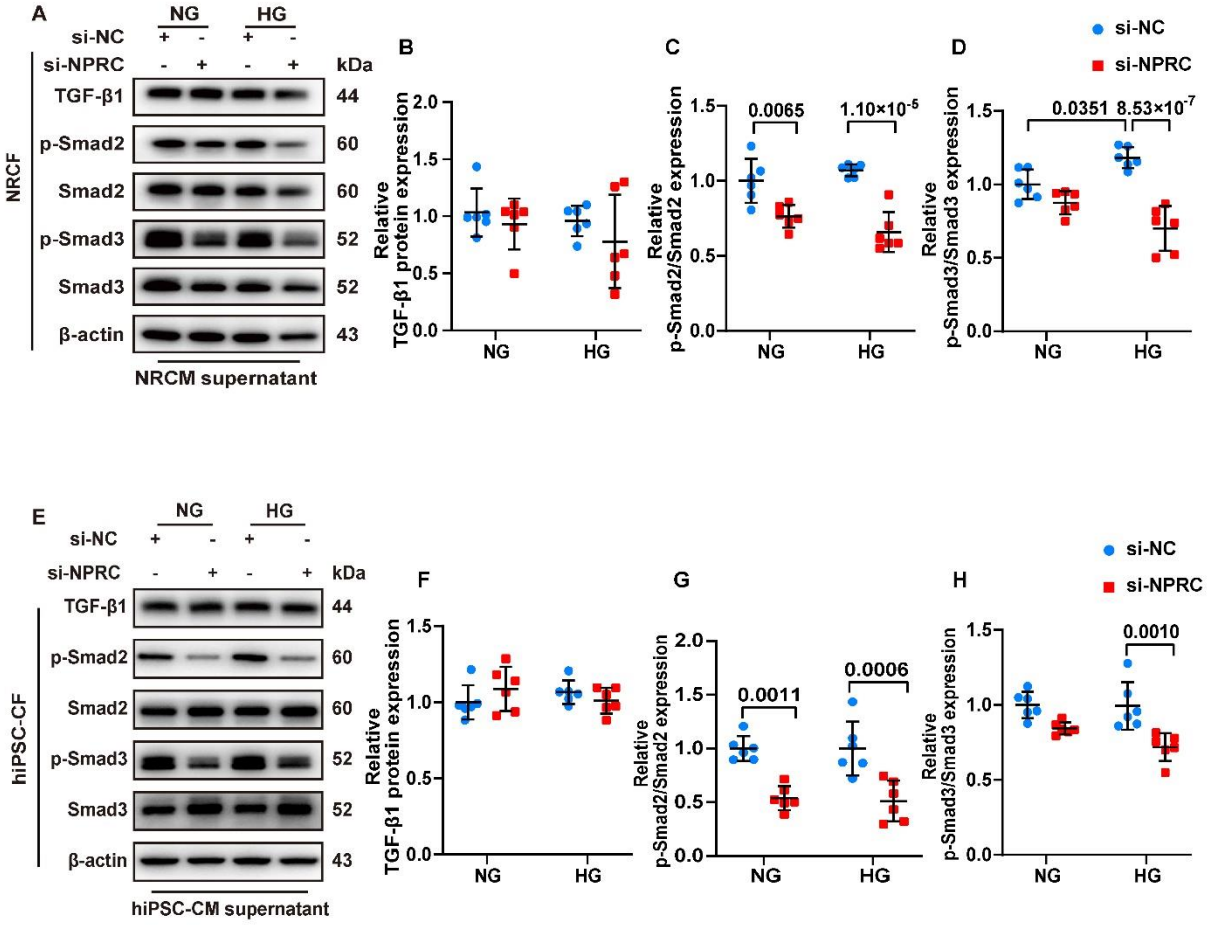

Fig. S11. NPRC deficiency in CMs inhibited TGF-β1/Smad signaling in CFs *in vitro.* (**A**) Representative Western blot images of TGF-β1, p-Smad2, and p-Smad3 expression in NRCFs treated with the supernatant of NRCMs that were transfected with si-NC or si-NPRC and treated with NG (5.5 mM) or HG (33.3 mM). (**B-D**) Quantification of the protein expression of TGF-β1, p-Smad2, and p-Smad3 in (**A**). n = 6 per group. (**E**) Representative Western blot images of TGF-β1, p-Smad2, and p-Smad3 expression in hiPSC-CFs treated with the supernatant of hiPSC-CMs that were transfected with si-NC or si-NPRC and treated with NG or HG. (**F-H**) Quantification of the protein expression of TGF-β1, p-Smad2, and p-Smad3 in (**E**). n = 6 per group. NG: normal glucose; HG: high glucose.

Normal distributions were tested by Shapiro-Wilk method. Two-way ANOVA with Turkey's post-hoc test was used in (**D**). Two-way ANOVA with Bonferroni post-hoc test was used in (**B-C, F-H**).

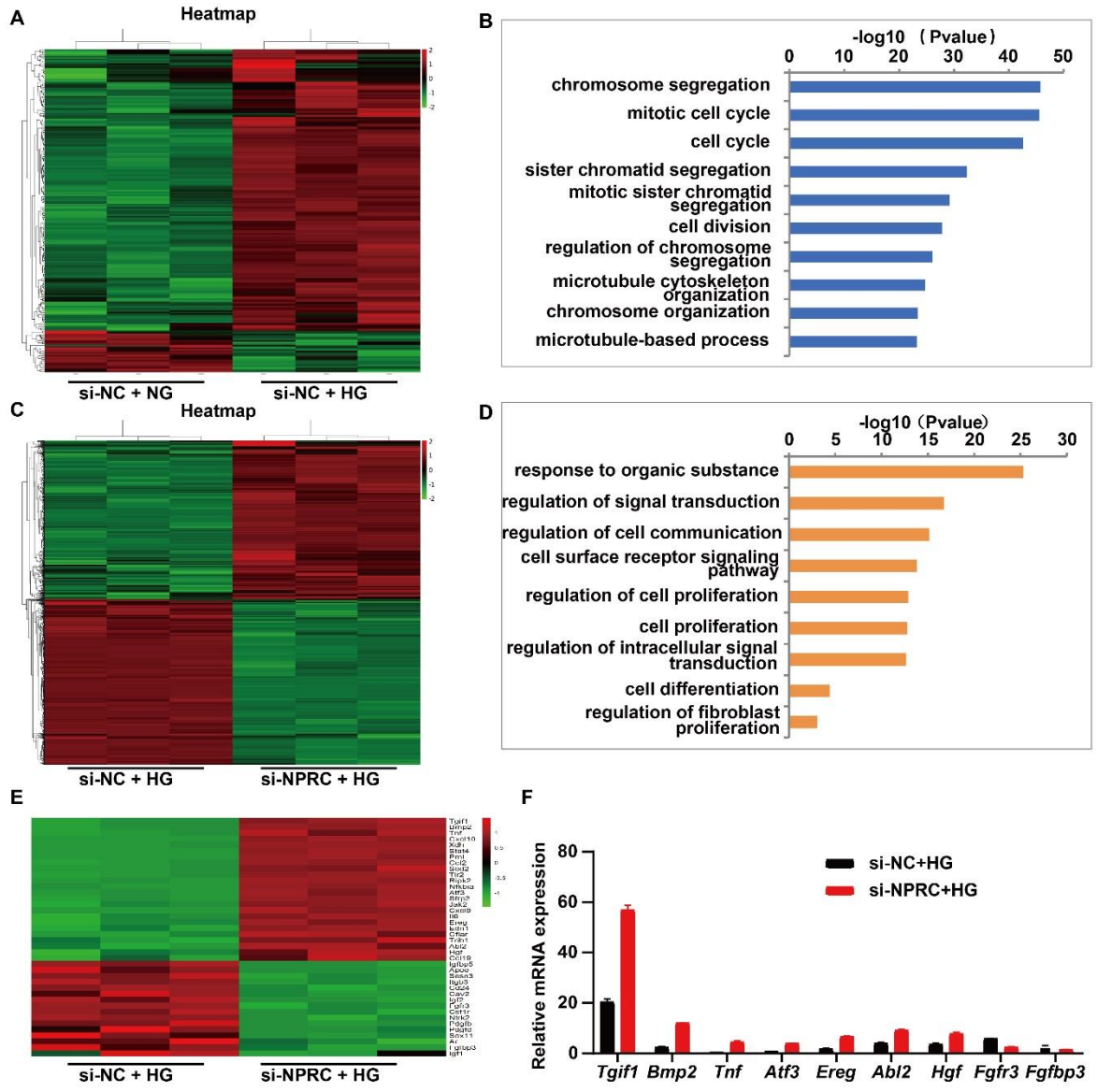

Fig. S12. Transcriptome profiles of the NRCFs transfected with si-NC or si-NPRC. (**A**) Hierarchical clustering heatmap of the differentially expressed genes in NRCFs treated with si-NC + NG or si-NC + HG. (**B**) Gene ontology (GO) enrichment of the differentially expressed genes in NRCFs treated with si-NC + NG or si-NC + HG. (**C**) Hierarchical clustering heatmap of the differentially expressed genes in NRCFs treated with si-NC + HG or si-NPRC + HG. (**D**) GO enrichment of the differentially expressed

genes in NRCFs treated with si-NC + HG or si-NPRC + HG. (**E**) Heatmap of the frequently repeated genes in GO enrichment in (**D**). (**F**) Relative mRNA expression and fold changes of fibrosis-related genes in (**E**). NG: normal glucose; HG: high glucose.

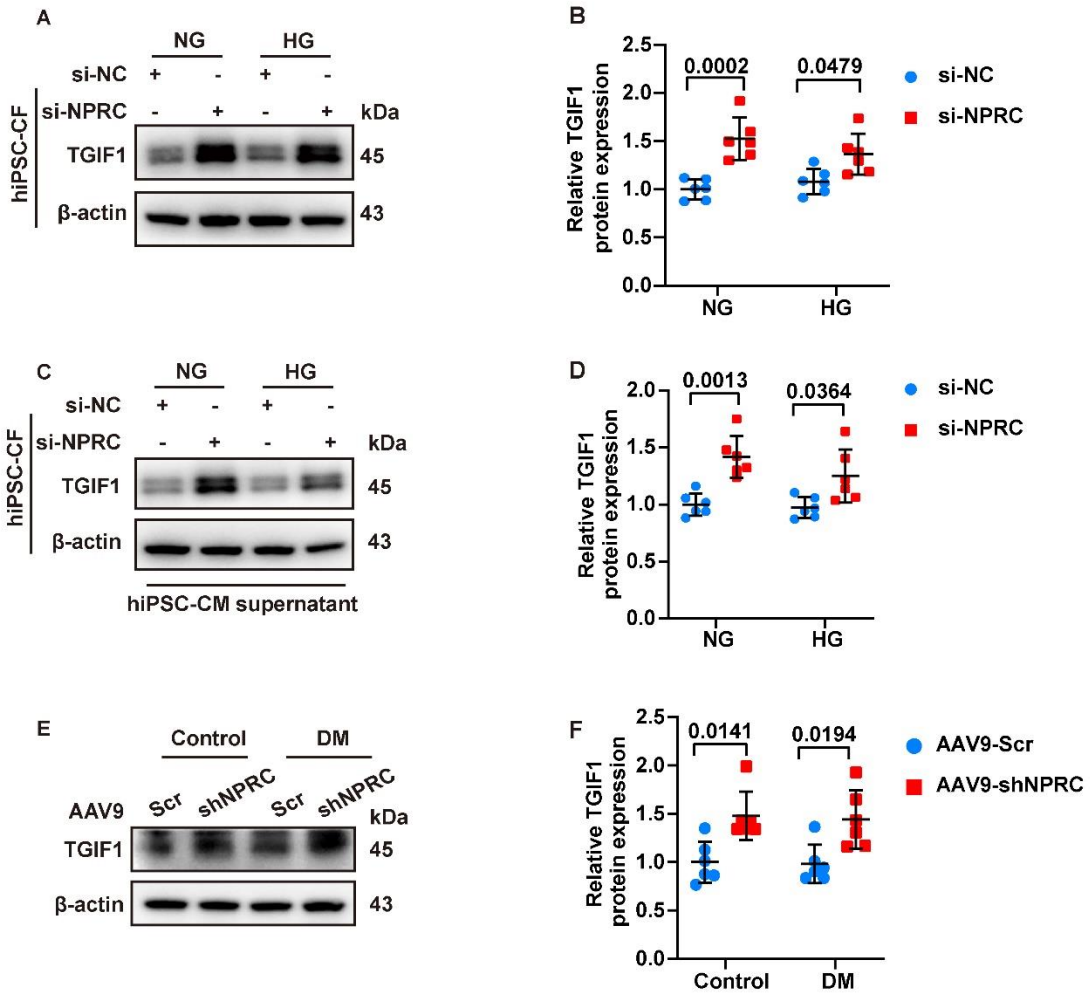

Fig. S13. NPRC deficiency increased TGIF1 expression *in vitro* and *in vivo*. (**A-B**) Representative Western blot images and quantification of the protein expression of TGIF1 in hiPSC-CFs transfected with si-NC or si-NPRC and treated with NG or HG. n = 6 per group. (**C-D**) Representative Western blot images and quantification of the protein expression of TGIF1 in hiPSC-CFs treated with the supernatant of hiPSC-CMs. n = 6 per group. (**E-F**) Representative Western blot images and quantification of the protein expression of TGIF1 in the hearts of AAV9-delivered mice. n = 6 per group. NG: normal

glucose; HG: high glucose. Normal distributions were tested by Shapiro-Wilk method. Two-way ANOVA with Bonferroni post-hoc test was used in (**B, D, and F**).

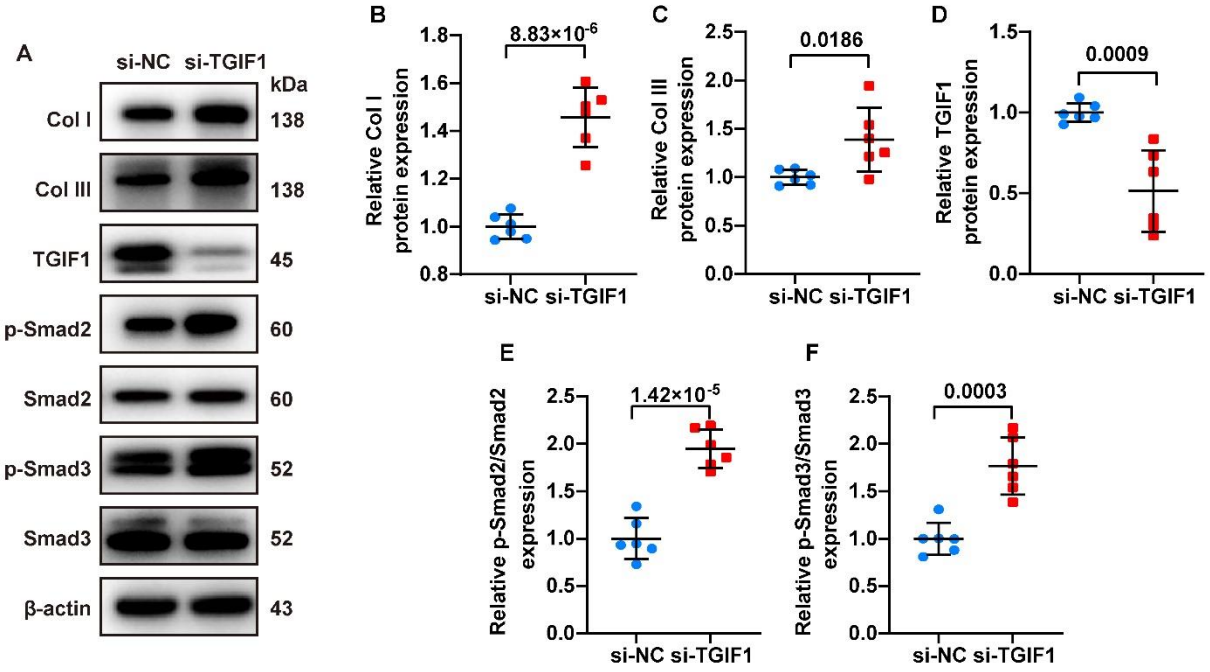

Fig. S14. Effect of TGIF1 knockdown on collagen synthesis and phosphorylation levels of Smad2/3 in NRCFs. (**A**) Representative Western blot images of collagen I, collagen III, TGIF1, p-Smad2, and p-Smad3 expression in NRCFs transfected with si-NC or si-TGIF1. (**B-F**) Quantification of the protein expression of collagen I, collagen III, TGIF1, p-Smad2, and p-Smad3 in NRCFs in (**A**). n = 6 per group. Normal distributions were tested by Shapiro-Wilk method. Unpaired two-tailed Student's t tests were applied in (**B-F**).

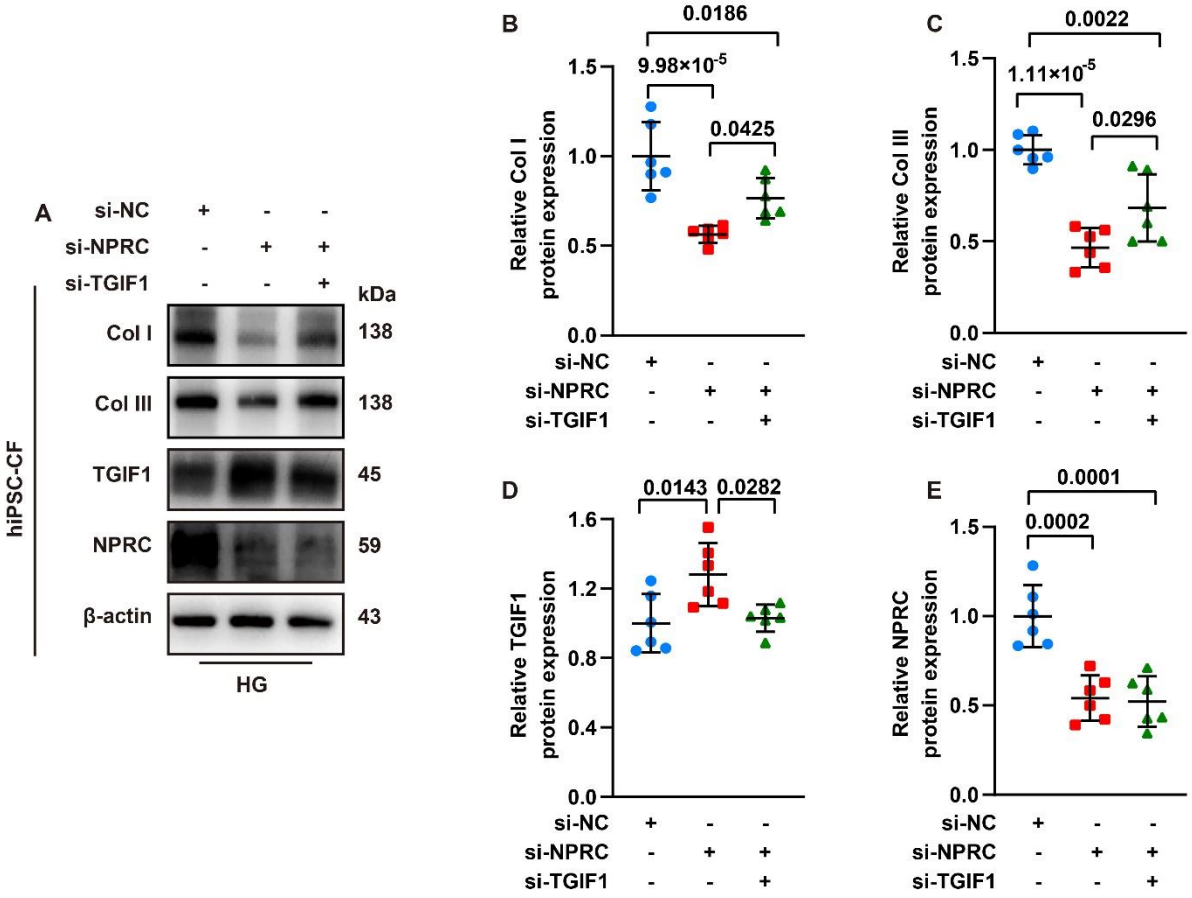

Fig. S15. TGIF1 mediated the effects of NPRC deficiency on collagen synthesis in hiPSC-CFs. (A). Representative Western blot images of collagen I, collagen III, TGIF1, and NPRC expression in hiPSC-CFs transfected with si-NC, si-NPRC, or si-NPRC + si-TGIF1. (**B-E**) Quantification of the protein expression of collagen I, collagen III, TGIF1, and NPRC in (**A**). n = 6 per group. Col I: Collagen I; Col III: Collagen III; Normal distributions were tested by Shapiro-Wilk method. One-way ANOVA was applied in (**B-E**).

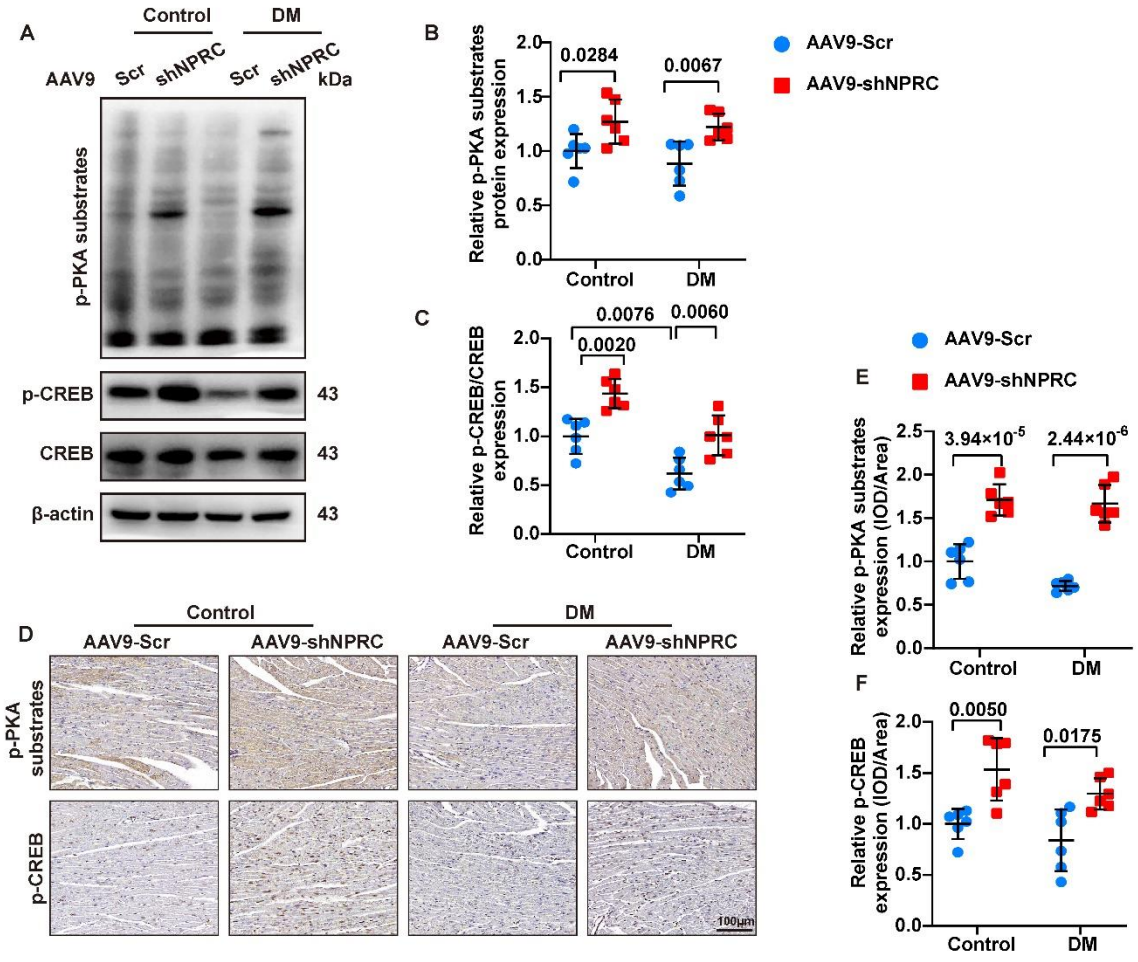

Fig. S16. Cardiac NPRC knockdown by AAV activated cAMP/PKA signaling *in vivo.* (**A**). Representative Western blot images of p-PKA substrates and p-CREB expression in the hearts of AAV9-delivered mice. (**B-C**) Quantification of the protein expression of p-PKA substrates and p-CREB in (**A**). n = 6 per group. (**D**) Representative IHC images of p-PKA substrates and p-CREB expression in the hearts of AAV9-delivered mice. Bar = 100 μm. (**E-F**) Quantification of the protein expression of p-PKA substrates and p-CREB in (**D**). n = 6 per group. DM: diabetes mellitus. Normal distributions were tested by Shapiro-Wilk method. Two-way ANOVA with Bonferroni post-hoc test was used in (**B-C**)**,** and (**E-F**)**.**

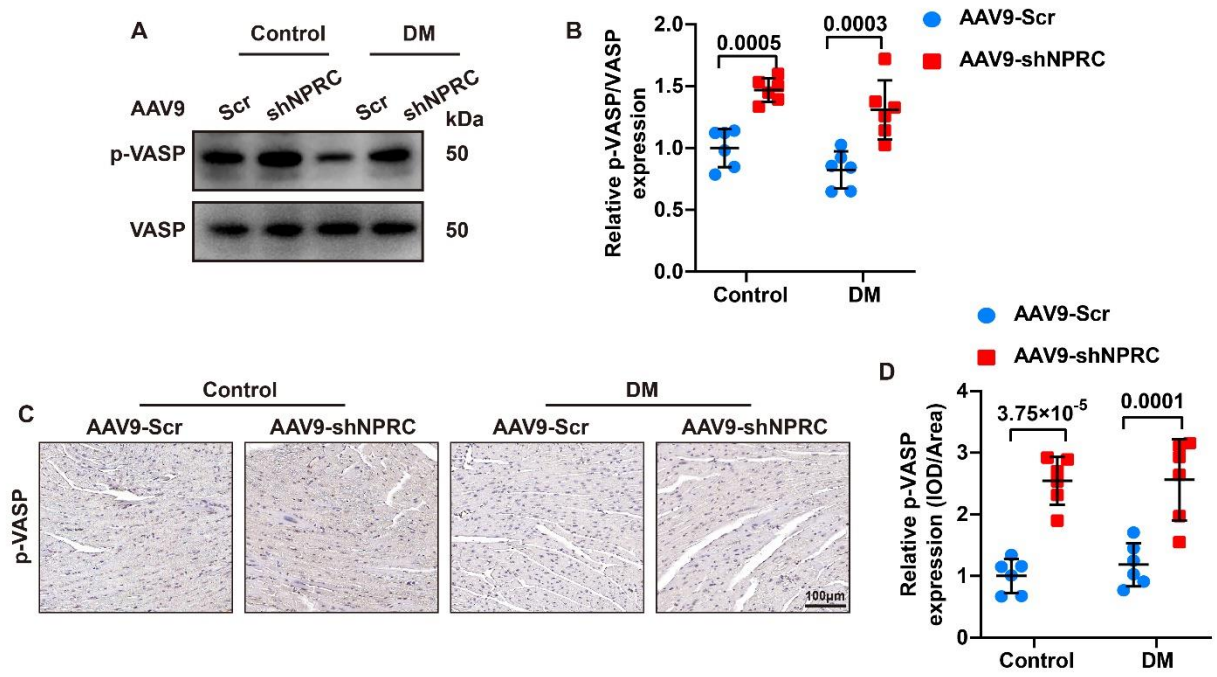

Fig. S17. Cardiac NPRC knockdown by AAV activated cGMP/PKG signaling *in vivo.* (**A**). Representative Western blot images of p-VASP expression in the hearts of AAV9-delivered mice. (**B**) Quantification of the protein expression of p-VASP in (**A**). n = 6 per group. (**C**) Representative IHC images of p-VASP expression in the hearts of AAV9-delivered mice. Bar = 100 μm. (**D**) Quantification of the protein expression of p-VASP in (**C**). n = 6 per group. DM: diabetes mellitus. Normal distributions were tested by Shapiro-Wilk method. Two-way ANOVA with Bonferroni post-hoc test was used in (**B**)**,** and (**D**)**.**

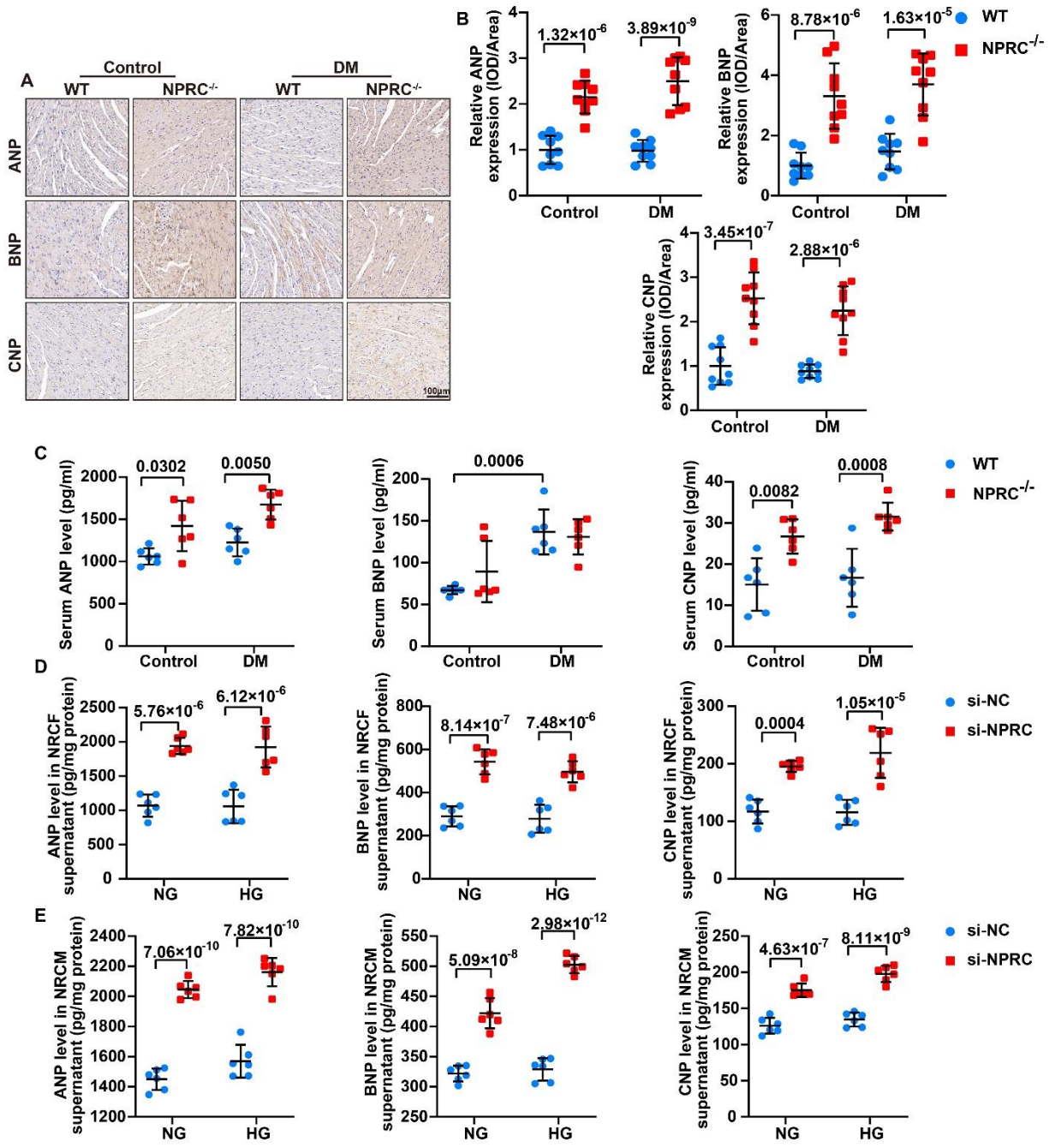

Fig. S18. NPRC deficiency increased NP levels *in vivo* and *in vitro*. (**A**) Representative IHC images of ANP, BNP, and CNP in the hearts of four groups of mice. Bar = 100 μm. (**B**) Quantification of IHC staining of ANP, BNP, and CNP in (**A**)**.** n = 9 per group. (**C**) Quantification of serum levels of ANP, BNP, and CNP in four groups of mice. n = 6 per group. (**D**) ANP, BNP, and CNP levels in cell supernatant of NRCFs transfected with si-NC or si-NPRC and treated with NG or HG. n = 6 per group. (**E**) ANP, BNP, and CNP levels in cell supernatant of NRCMs transfected with si-NC or si-NPRC and treated

with NG or HG. n = 6 per group. DM: diabetes mellitus; NG: normal glucose; HG: high glucose. Normal distributions were tested by Shapiro-Wilk method. Two-way ANOVA with Bonferroni post-hoc test was used in (**B-E**)**.**

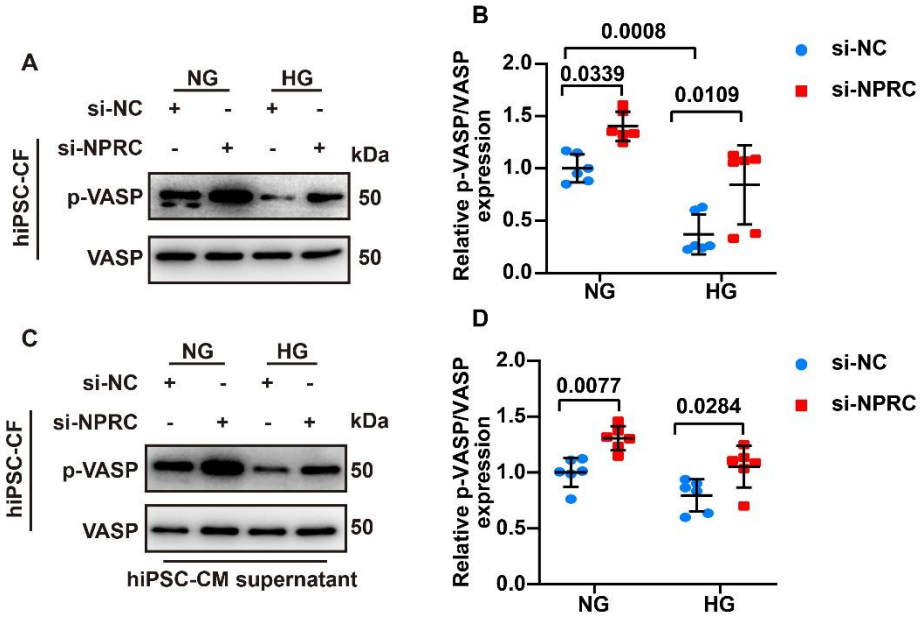

Fig. S19. NPRC deficiency activated cGMP/PKG signaling in hiPSC-CFs. (**A-B**) Representative Western blot images and quantification of the protein expression of p-VASP in hiPSC-CFs transfected with si-NC or si-NPRC and treated with NG or HG. n = 6 per group. (**C-D**) Representative Western blot images and quantification of the protein expression of p-VASP in hiPSC-CFs treated with the supernatant of hiPSC-CMs. n = 6 per group. NG: normal glucose; HG: high glucose. Normal distributions were tested by Shapiro-Wilk method. Two-way ANOVA with Bonferroni post-hoc test was used in (**B**)**,** and (**D**)**.**

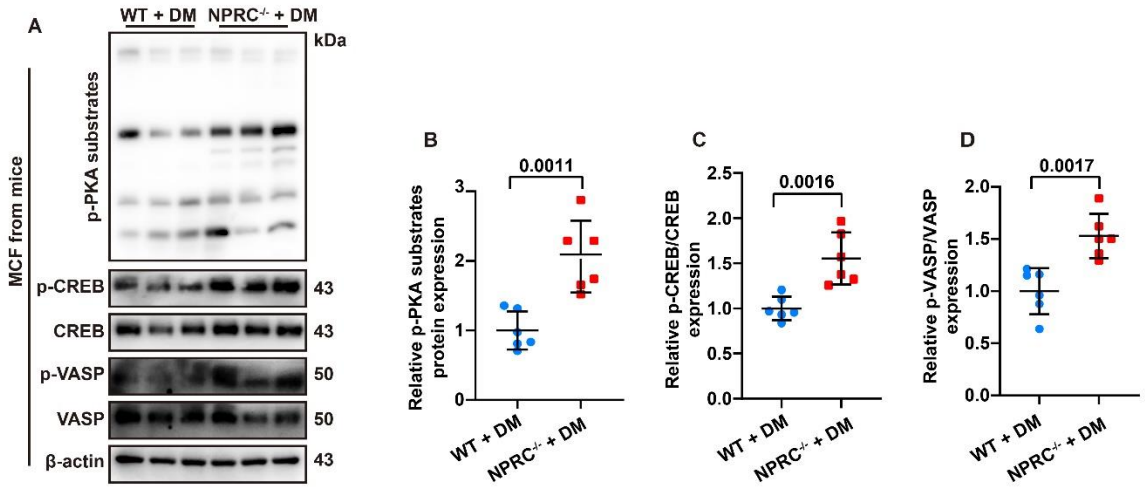

Fig. S20. NPRC deficiency activated cAMP/PKA and cGMP/PKG signaling in adult mouse CFs (MCF). (A). Representative Western blot images of p-PKA substrates, p-CREB, and p-VASP of adult MCFs isolated from the hearts of diabetic WT and NPRC$^{-/-}$ mice. (**B-D**). Quantification of the protein expression of p-PKA substrates, p-CREB, and p-VASP in (**A**). n = 6 per group. DM: diabetes mellitus; Normal distributions were tested by Shapiro-Wilk method. Unpaired two-tailed Student's t tests were applied in (**B-D**).

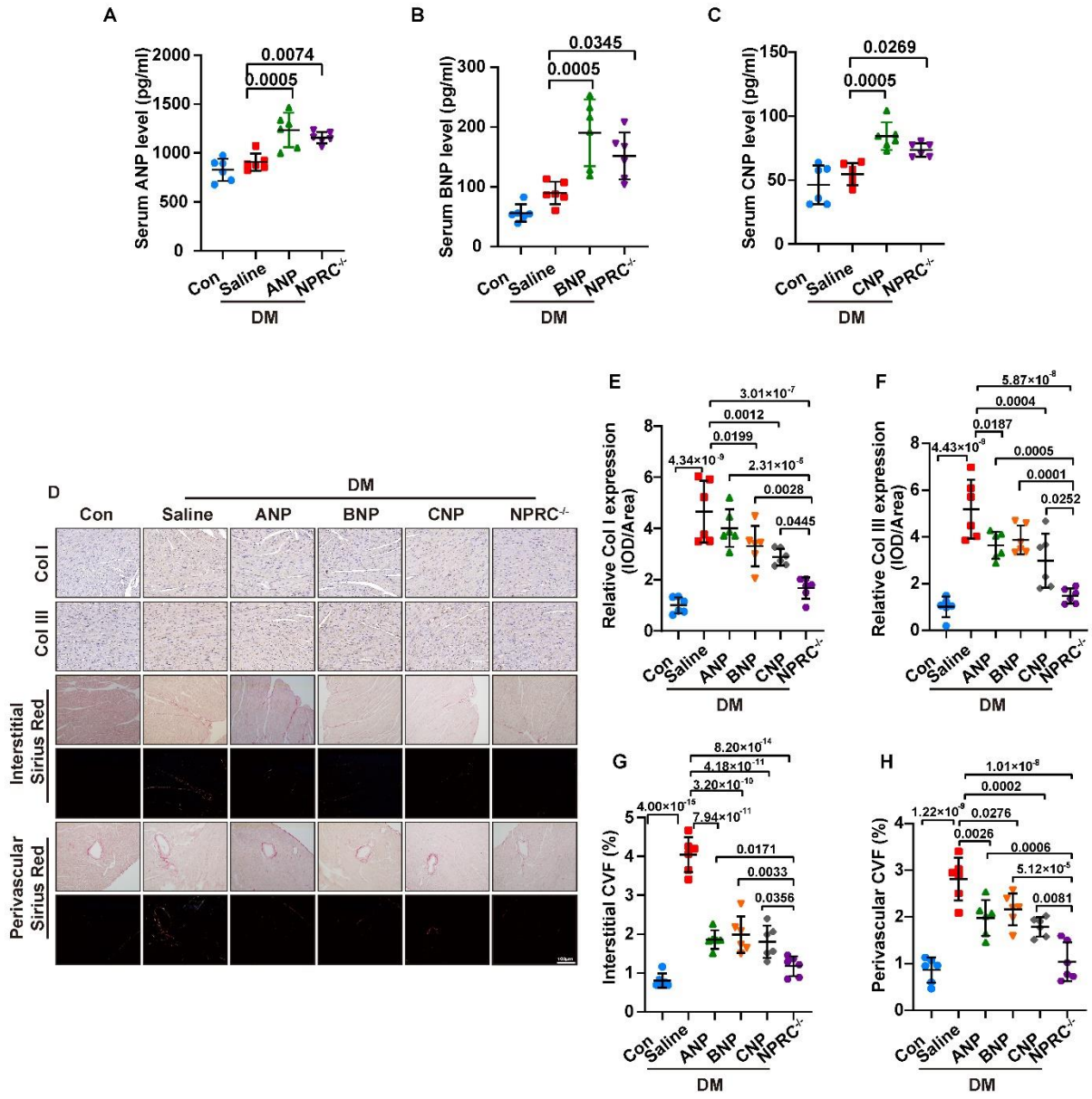

Fig. S21. Comparison of cardioprotective effects between NPRC deletion and ANP, BNP, or CNP infusion in diabetic mice. (**A**) Serum levels of ANP in Con, DM + Saline, DM + ANP, and DM + NPRC$^{-/-}$ mice. (**B**) Serum levels of BNP in Con, DM + Saline, DM + BNP, and DM + NPRC$^{-/-}$ mice. (**C**) Serum levels of CNP in Con, DM + Saline, DM + CNP, and DM + NPRC$^{-/-}$ mice. n = 6 per group. (**D**)**.** Representative images of IHC (collagen I and collagen III on the first and the second row) and the Sirius red staining (the third to the bottom row) of the myocardium in six groups of mice. Bar = 100 μm. (**E-H**) Quantification of collagen I and collagen III expression, interstitial collagen volume

fraction (CVF), and perivascular CVF in (**D**). Col I: Collagen I; Col III: Collagen III. Normal distributions were tested by Shapiro-Wilk method. One-way ANOVA was used**.**

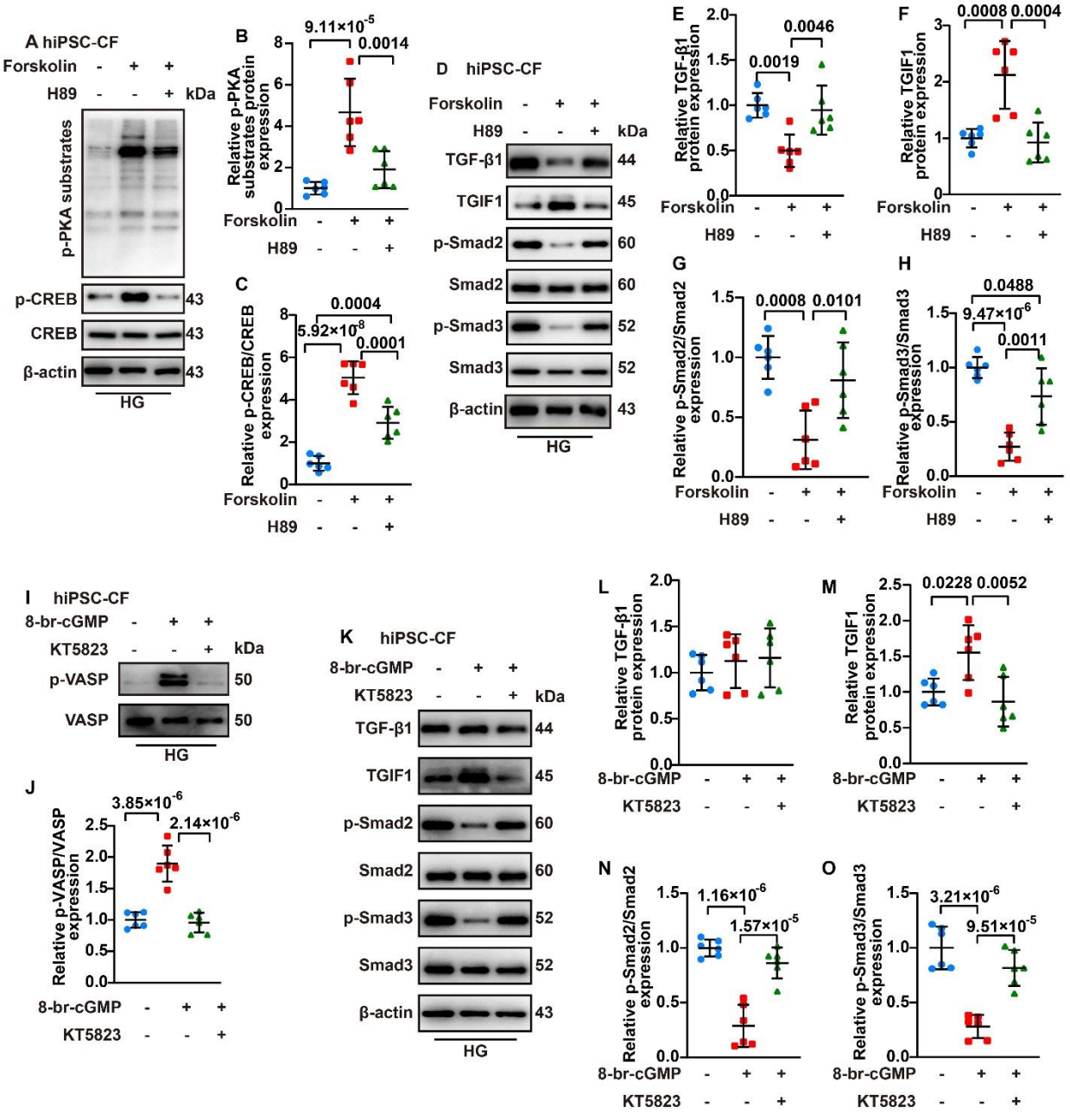

Fig. S22. Activation of cAMP/PKA or cGMP/PKG signaling increased TGIF1 expression but cAMP/PKA activation inhibited TGF-β1 expression in hiPSC-CFs. (**A**) Representative Western blot images of p-PKA substrates and p-CREB expression in

hiPSC-CFs which were treated with either forskolin or forskolin combined with H89 followed by HG treatment. (**B-C**) Quantification of the protein expression of p-PKA substrates and p-CREB in (**A**). n = 6 per group. (**D**) Representative Western blot images of TGF-β1, TGIF1, p-Smad2, and p-Smad3 expression in hiPSC-CFs which were treated with either forskolin or forskolin combined with H89 followed by HG treatment. (**E-H**) Quantification of the protein expression of TGF-β1, TGIF1, p-Smad2, and p-Smad3 in (**D**). n = 6 per group. (**I**) Representative Western blot images of p-VASP in hiPSC-CFs treated with either 8-br-cGMP or 8-br-cGMP combined with KT5823 followed by HG treatment. (**J**) Quantification of the protein expression of p-VASP in (**I**). n = 6 per group. (**K**) Representative Western blot images of TGF-β1, TGIF1, p-Smad2, and p-Smad3 expression in hiPSC-CFs treated with either 8-br-cGMP or 8-br-cGMP combined with KT5823 followed by HG treatment. (**L-O**) Quantification of the protein expression of TGF-β1, TGIF1, p-Smad2, and p-Smad3 in (**K**). n = 6 per group. HG: high glucose. Normal distributions were tested by Shapiro-Wilk method. One-Way ANOVA was used in (**B-C, E-H, J,** and **L-O**).

Table S1. Antibodies and manufacturers

Antibody	Company	Catalog NO.	Concentrations
NPRC	GeneTex	GTX110023	WB: 1:1000
			IF: 1:200
	Origene	TA500956	WB: 1:1000
GCA	GeneTex	GTX14918	WB: 1:1000
GCA	GeneTex	GTX109810	IF: 1:200
GCB	Origene	TA351444	WB: 1:1000
			IF: 1:200
Collagen I	Proteintech	66761-1-Ig	WB: 1:1000
Collagen I	Abcam	ab34710	IHC: 1:200
Collagen III	Proteintech	22734-1-AP	WB: 1:1000
Collagen III	Abcam	ab7778	IHC: 1:200
TGF-β1	Abcam	ab215715	WB: 1:1000
TGFβR2	Proteintech	66636-1-Ig	WB: 1:1000
p-Smad2	Cell Signaling Technology	3108	WB: 1:1000
Smad2	Cell Signaling Technology	5339	WB: 1:1000
p-Smad3	Cell Signaling Technology	9520	WB: 1:1000
Smad3	Cell Signaling Technology	9523	WB: 1:1000
PCNA	SantaCruz	sc-56	WB: 1:100
TGIF1	Abcam	ab52955	WB: 1:1000
cPML	Abcam	ab179466	WB: 1:1000
			IF: 1:200
cPML	SantaCruz	sc-377390	IP: 1μg/ml
Lamin B	Proteintech	12987-1-AP	WB: 1:1000
p-PKA	Cell Signaling Technology	9621	WB: 1:1000
substrates			IHC: 1:200
p-CREB	Cell Signaling Technology	9198	WB: 1:1000
			IHC: 1:500
CREB	Cell Signaling Technology	9197	WB: 1:1000
p-VASP	Cell Signaling Technology	3114	WB: 1:1000

p-VASP	Abcam	ab194747	IHC: 1:200
VASP	Cell Signaling Technology	3112	WB: 1:1000
ANP	GeneTex	GTX109255	IHC: 1:200
BNP	Abcam	ab243400	IHC: 1:200
CNP	Genetax	GTX55996	IHC: 1:200
β-actin	Abcam	ab8227	WB: 1:1000

Table S2. Sequence of primers and siRNAs

Primers	**Sequence (5'-3')**
npr3	forward: ATCGAGAGCTGCGGGAAGAT
	reverse: TCAAGCAGACAAAGCAAGGG
npr1	forward: CATTGAGCGTGTGACTCGGG
	reverse: GCGAATCTGCTGAAAGGGTG
npr2	forward: TGGGCACGGGAATCACTTTC
	reverse: GAGCGAGCCGTAACTGGAT
tgif1	forward: TCAGTTCACCATTTCCCGCC
	reverse: GGAGGTTTGGGAGACACTGG
β-actin	forward: GCAGGAGTACGATGAGTCCG
	reverse: ACGCAGCTCAGTAACAGTCC
siRNAs	**Sequence (5'-3')**
negative control	UUCUCCGAACGUGUCACGUTT
NPRC (SR502884A)	GCUCUACAGCGACGACAAACUCGAG
NPRC (SR502884B)	GCGAUCCAAUGUCAAAUAUCCUUGG
NPRC (SR502884C)	GGCCUAGAAGAAUCAGCAGUGACAG
TGIF1	UGUUGUUGCAGCAGCAUUUTT